The Journal of Experimental Biology 210, 3328-3336
Published by The Company of Biologists 2007
doi:10.1242/jeb.008292

Timing is everything: coordination of strike kinematics affects the force exerted by suction feeding fish on attached prey

Roi Holzman[1,*], Steven W. Day[2] and Peter C. Wainwright[1]

[1]*Section of Evolution and Ecology, University of California, One Shields Avenue, Davis, CA 95616, USA and* [2]*Department of Mechanical Engineering, Rochester Institute of Technology, 76 Lomb Memorial Drive, Rochester, NY 14623-5604, USA*

*Author for correspondence (e-mail: raholzman@ucdavis.edu)

Accepted 17 July 2007

Summary

During aquatic suction feeding, the predator opens its mouth and rapidly expands its buccal cavity, generating a flow field external to the mouth. The rapid expansion of the buccal cavity produces high fluid velocities and accelerations that extend only a short distance from the mouth (about half of one mouth diameter), and only persist for several milliseconds. Therefore, the predator must precisely time its strike to locate the prey within the narrow region of high flow, during the brief period when flow is at its peak. With flow being the agent for transferring force to the prey, the predator may enhance these forces by producing higher water velocities and faster acceleration at the mouth, but also through increasing the strike's accuracy, i.e. locating the prey closer to the mouth at the instant of peak flow speed. The objectives of this study were to directly measure forces exerted by bluegill *Lepomis macrochirus* on their prey and to determine how bluegill modify force output. Bluegill were offered ghost shrimp tethered to a load cell that recorded force at 5000 Hz, and feeding sequences were synchronously recorded using 500 Hz video. Peak forces exerted on attached 20 mm shrimp ranged from 0.005 N to 0.506 N. In accordance with the short duration of the strikes (average time to peak gape of ~13 ms), the forces recorded were brief (~12 ms from initiation to peak force), and force magnitude declined rapidly after peak force. Statistical analysis indicated that rate of buccal expansion, and prey size, but not strike initiation distance, significantly affected peak force. These observed variables were used with results from flow visualization studies to estimate the flow at the prey's location, which allowed the calculation of drag, pressure gradient force and acceleration reaction force. The relationship between these calculated forces and the measured forces was strong, indicating that the model can be used to estimate forces from strike kinematics. This model was then used to study the effects of strike initiation distance on peak force and on the rate of increasing force. Comparisons of model output to empirical results indicated that bluegill time their strike so as to exert an average of ~70% of the peak possible force on the prey, and that the observed strike initiation distance corresponded to the distance that maximized modeled force on an attached prey. Our results highlight the ability of bluegill to produce high forces on their prey, and indicate that precision and visual acuity play important roles in prey acquisition, beyond their recognized role in prey detection.

Key words: *Lepomis macrochirus*, kinematics, prey capture, strike performance accuracy, suction feeding, force.

Introduction

Suction feeding is a behavior unique to the aquatic environment, in which fish exert force on a prey item that is outside their immediate reach by manipulating water flow around it (Wainwright and Day, 2007). Unless the fish also swims forward quickly during the strike, the success of the strike depends on applying suction force to draw the prey into the mouth. When feeding on evasive prey, a suction feeding fish must exert sufficient force, through strong flow speed and fast accelerations, to overcome any escape attempt by the prey (Wainwright and Day, 2007). If the prey is attached to the substrate, higher force increases the chance of detaching it (Denny et al., 1985). In spite of its central role in prey capture by suction feeders, force has rarely been identified as an indicator of suction performance, and direct measurements have not been reported in the literature.

The flow produced by suction feeding fishes is used to exert force on an object outside their physical reach. Bluegill *Lepomis macrochirus* are capable of generating flows as fast as 2.5 m s^{-1} (Day et al., 2005; Higham et al., 2006a). Flow speed in this species is correlated with the speed of mouth expansion, increasing with faster times to peak gape (TTPG) and decreasing with distance from the mouth (Day et al., 2005; Higham et al., 2006a). During the strike, high flow velocity only persists for about 10 ms (Day et al., 2005; Higham et al., 2006a). Moreover, a trade-off exists between the magnitude of peak flow (faster flows with shorter TTPG) (Day et al., 2005) and peak flow duration (longer with longer TTPG).

In order to maximize the forces exerted on the prey by the suction flow, the predator must precisely coordinate its strikes so that the prey is positioned near the mouth at the time of highest flow. The ephemeral nature of the suction flow suggests that the window of time when maximum forces can be exerted only lasts a few milliseconds. It follows, then, that there will be an optimal timing and positioning that maximizes the force exerted on the prey. These optima can differ between individual strikes, which differ in their peak flow speeds and accelerations, strike initiation distances, the distance closed between the predator and the prey during the strike, and other aspects of strike kinematics. While bluegill are consistent in positioning their prey in the center of the water parcel they engulf during the strike (Higham et al., 2006a), it is not known whether that consistency maximizes the force that is exerted on the prey.

The role of morphology and size in determining suction feeding performance has received much attention (Carroll et al., 2004; Norton, 1991; Van Wassenbergh et al., 2006). Likewise, it is recognized that predators can modify their prey capture kinematics in response to prey type (Coughlin and Strickler, 1990; Norton, 1991; Wainwright et al., 2001), inducing faster buccal expansion when feeding on evasive prey (Coughlin and Strickler, 1990; Wainwright et al., 2001). However, previous researchers have not explored the potential synergy gained from coordination among the kinematic events of the strike with respect to the forces exerted on the prey.

The objectives of this study were twofold: to measure the force exerted by a suction-feeding fish on an attached prey and to determine how effective the fish was at timing the initiation of the strike to maximize the force exerted on the prey. Forces were measured by allowing the fish to strike on shrimp attached to a small force transducer. Analyses of strike kinematics were used to estimate temporal and spatial patterns of water flow, which were used in calculations of the peak forces that bluegill exert on prey [based on a model by Wainwright and Day (Wainwright and Day, 2007)]. That model was subsequently used to calculate the peak force that would be produced with varying strike initiation distances, in order to compare the force exerted at the observed distance to that exerted at the optimal initiation distance. This approach allows us to evaluate the ability of bluegill to coordinate the timing of the onset of the strike with the profile of kinematics in each strike in a way that maximizes the force exerted on the prey item. In this study we focus on a scenario where the prey does not try to escape from the feeding fish, but instead resists the force exerted by the suction feeder by gripping the substratum. While encounter scenarios with free moving prey may result in different strategies by the predator, the fixed prey situation occurs frequently in nature.

Materials and methods

Bluegill *Lepomis macrochirus* (Rafinesque), a member of the Centrarchidae, were selected for this study because they are often considered highly specialized suction feeders (Carroll et al., 2004) and have been the focus of considerable previous research on suction feeding (Carroll et al., 2004; Day et al., 2005; Ferry-Graham et al., 2003; Gibb and Ferry-Graham, 2005; Gillis and Lauder, 1995; Higham et al., 2005; Higham et al., 2006b). These fish feed on a variety of prey types, including several that rely on crypsis to avoid detection and may defend themselves by gripping the rocks, wood or vegetation they live on. Many species of Odonata larvae, Trichoptera nymphs and Ephemeroptera larvae and gastropods fit this profile (Flemer and Woolcott, 1966; Huish, 1957; Sadzikowski and Wallace, 1976; VanderKooy et al., 2000). Fish were caught locally in Yolo County, near Davis, CA, USA, and housed in 100-liter aquaria at 22°C. The fish were fed daily with pieces of squid (*Loligo* spp.), live ghost shrimps (*Palaemonetes* spp.), and annelid worms. The fish were trained to feed in the experimental setup (see below; Fig. 1) for at least a week before the experiments began. We analyzed data from four individuals (standard length *SL*=167 mm, 178 mm, 172 mm, 156 mm) while feeding on ghost shrimps (*Palaemonetes*; size range 20±1 mm).

Experimental protocol and force measurements

The fish were starved for 24 h before each experimental day. At the onset of each experimental trial, the fish was held in the far side of an aquarium by a trap door. When the door was opened, the fish was permitted to move across the aquarium and capture its prey. The location of the door ensured that the fish approached the prey horizontally, and that the strike trajectory would be at a right angle to a video camera (Fig. 1). The fish were filmed during the approach to the prey in lateral view using a high-speed digital video camera (500 frames s^{-1}, NAC Memrecam Ci, Japan). We define the strike as the sequence of events during feeding from the beginning of mouth opening until the mouth is closed again.

The prey, live ghost shrimp, were stretched out and their ventral surface was glued with a cyanoacrylate adhesive to a metal wire (0.3 mm in diameter) protruding from a load cell (Futek S-Beam Jr load cell 1 lb, Irvine, CA, USA). The output of the load cell (voltage) was recorded at 5000 Hz on a PC running a custom LabView script through a DAQpad 6070E data acquisition system (National Instruments, Austin, TX, USA). The camera and the load cell were synchronized using an external trigger. Conversion of voltage data to force was based on factory calibration of the load cell, which was verified independently using a series of measured weights before each experimental day. The sensitivity of the load cell, combined with the data acquisition system was 0.001 N in the range of 0–4.44 N.

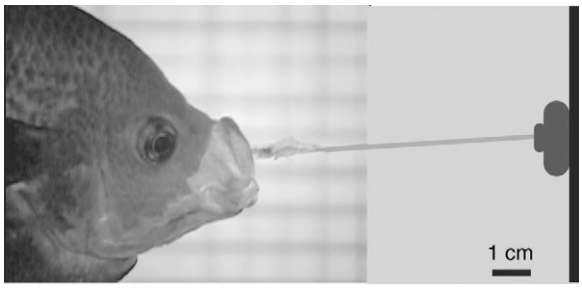

Fig. 1. Photograph of a bluegill striking at a tethered shrimp. The picture was taken at time of peak gape (95% of maximal gape). The shrimp was glued to a thin metal rod that was extended from a load cell (shown as a black oval) that recorded data at 5000 Hz. Synchronized video recordings were made at 500 Hz.

Video sequences taken during feeding events were downloaded to a PC and analyzed using ImageJ version 1.33 (NIH, Bethesda, MD, USA). For each sequence, we analyzed each frame starting ~10 frames before the onset of gape expansion and ending ~10 frames after the fish started closing its mouth (Fig. 2A). For each frame, the *x* and *y* coordinates of the position of the fish's upper and lower jaw (at their most anterior end) and the prey's eye were determined. These three landmarks were used to calculate the following variables: gape distance, the distance between the predator and prey (defined as the distance between the center of the bluegill's mouth and the eye of the prey), as well as mouth displacement, defined as the displacement of the center of the mouth on the predator–prey axis (the imaginary line connecting the prey and the fish at the initiation of the strike). For each sequence we also determined the time to peak gape (TTPG), defined as the time it took the fish to open its mouth from 20% to 95% of the maximal gape observed during the strike (see Day et al., 2005; Sanford and Wainwright, 2002), the distance between the center of the fish's mouth and the prey at the time of strike initiation (the onset of gape increase), the size of peak gape, prey length and maximal prey diameter (maximal height in lateral view). Peak flow speed at the mouth was estimated for each strike based on the relationship between TTPG and peak flow speed (see Day et al., 2005). The force measured at each frame was averaged for the three consecutive force readings at –0.2, 0 and +0.2 ms relative to the timing of the frame (to temporally coordinate the samples taken by the camera and the force transducer). Twelve strikes were analyzed for each of the four fish. Strikes were included in the analyses only if there was no contact between the prey and the bluegill's jaws prior to mouth closing, and only if the prey remained attached to the transducer through the strike.

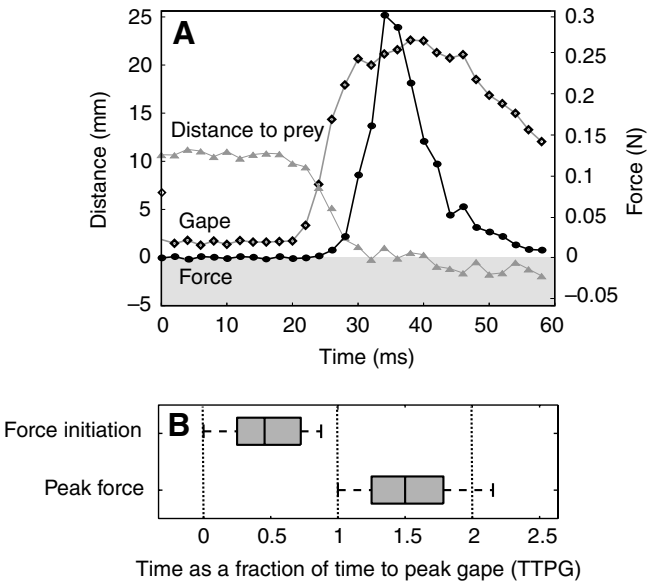

Fig. 2. (A) The change in observed force (filled circles), gape size (open diamonds) and distance to the prey (gray triangles) during a representative strike. The distance between the prey and the fish is closed by rapid forward movement of the jaws that occurs during mouth opening. Note that the initiation and peak of force lag the onset and peak of gape expansion, respectively. Grey area represents negative distances, i.e. where the prey is in the fish's mouth. (B) Temporal patterns for the force exerted on shrimp prey by bluegill sunfish. Time is given as a fraction of TTPG, defined as the duration from 20% to 95% of peak gape (0 to 1, respectively). The boxes have vertical lines at the lower quartile, median and upper quartile values. Whiskers represent the range for 95% of the observed values. *N*=48 strikes, 12 per fish.

Calculations of the forces exerted on a prey item

If the temporal and spatial pattern of water flow is known, along with some features of the prey item, then the forces exerted by the flow on the prey item can be calculated (Wainwright and Day, 2007). In general, the flow of water around an immersed object exerts three forces: drag, pressure gradient force and acceleration reaction (Batchelor, 1967; Denny, 1988; Wainwright and Day, 2007). Drag is exerted due to the movement of the fluid relative to the object (Batchelor, 1967; Denny, 1988; Wainwright and Day, 2007). The magnitude of drag depends on the prey's drag coefficient and size, and on relative flow speed squared. Pressure gradient force is the consequence of spatial and temporal gradients in flow velocity (Batchelor, 1967; Denny, 1988; Wainwright and Day, 2007). In a suction feeding fish, the flow speed in front of the mouth decreases non-linearly with the distance from the mouth (Day et al., 2005). Therefore, the upstream end of the prey is located in a region of relatively high flow velocity, and thus, lower pressure. The pressure gradient force scales with prey volume and with the magnitude of pressure gradient. The acceleration of flow around the prey generates an acceleration reaction (Batchelor, 1967; Vogel, 1994; Wainwright and Day, 2007), which is a function of prey volume and shape (the latter denoted by the object-specific added mass coefficient), the density of the water, and of the magnitude of relative fluid acceleration.

A function describing the change in gape as a function of time was fitted to empirical gape measurements for each individual sequence (see Muller et al., 1982). That function describes gape kinematics using six discrete variables: initial and peak gape, time of gape initiation and time of peak gape, α (a form coefficient for the rate of gape increase) and the amount of time spent at peak gape (Muller et al., 1982) (see Table 1). Similar functions were fitted to describe the position of the mouth as a function of time (mouth displacement) and to describe speed at the mouth as a function of time (Table 1). Time of flow initiation and peak flow speed were set to equal the time of 20% and 95% of peak gape (see Day et al., 2005). Initial flow speed was 0, and peak flow speed was estimated based on TTPG using the relationships found in Day et al. [(Day et al., 2005), see their fig. 9] for similar-sized bluegill. The form coefficient α for flow speed was equated to that of the gape, with no plateau in flow speed (i.e. flow decreasing after peak flow speed). Forces were calculated at time increments of 0.03 ms based on the resulting continuous function fit to the observed kinematics of gape and mouth displacement (see Table 1 for a complete list of variables used in the model).

The flow in front of the mouth of a suction-feeding fish decreases rapidly with the distance from the mouth (Day et al., 2005; Ferry-Graham et al., 2003; Higham et al., 2006a; Nauwelaerts et al., 2007). Therefore, for an elongate prey positioned with its long axis normal to the mouth opening (such

Table 1. *Parameters used in the calculation of forces exerted on the prey*

Input variables	Parameters	Source
t_{nul}, t_{max}, h_{nul}, h_{max}, α, plateau	Change in gape size with time	Fitted for each sequence based on observed kinematics
t_{nul}, t_{max}, h_{nul}, h_{max}, α, plateau	Change in mouth displacement with time	Fitted for each sequence based on observed kinematics
t_{nul}, t_{max}, h_{nul}, h_{max}, α, plateau	Change in flow speed with time	Estimated based on gape kinematics
	C_d, Re=300–10 000	Based on Kils (Kils, 1982)*
	C_d, Re=10 000–85 000	Measured
	Added mass coefficient (C_{am})	Estimated based on the fit of observed and calculated force
	Strike initiation distance	Measured
	Prey length	Measured
	Prey diameter	Measured
	Prey volume	Calculated based on length and diameter

*Based on measurements for *Euphausia superba*, similar in size and shape to ghost shrimps.

Parameters were recalculated for each strike, based on observed kinematics. Definition of input variables, used to calculate continuous functions for gape, mouth displacement and flow speed, followed Muller et al. (Muller et al., 1982): t_{nul}, initial value of the kinematic variable of interest; t_{max}, peak value; h_{nul}, time of initiation (first deviation from t_{nul}); h_{max}, time of peak value; α, a form coefficient for the rate of increase; plateau, the amount of time spent at peak value; C_d, drag coefficient (based on wetted area); Re, Reynolds number. The temporal patterns in flow speed were estimated based the relationships observed by Day et al. (Day et al., 2005).

as our 20 mm shrimp), the flow speed and acceleration will change as a function of the position along the anterior–posterior axis. To account for the change in flow pattern along that axis, we integrated the force along the anterior–posterior axis of the prey in 2 mm bins, summing the forces that act on the bins at each time step. The flow speed at each bin was calculated for each time step based on the distance between the center of the bin and the mouth. The volume and wetted area for each bin were calculated, assuming a cylindrical shape for each bin, with a diameter that was a function of the bin's position along the anterior–posterior axis. For each bin, the wetted area was defined based on its position; it included the cylindrical envelope in all the bins (calculated as the product of the bin's circumference and height) and, only for the proximal and distal bins, the frontal area of the cylinder. For each shrimp in the experiment, we measured the maximal diameter (maximal height in a lateral view, Fig. 1) and estimated the diameter at each bin based on the average proportional height at that bin. A consensus profile of height *vs* length of a stretched shrimp was obtained by measuring the cross-sectional height of five individual shrimp at multiple locations along the anterior posterior axis.

Drag force, F_d (N), acting on each bin was calculated as:

$$F_d = 0.5 \times C_d \times A_w \times \rho \times (FS)^2 ,$$

where C_d is an empirically determined drag coefficient (dimensionless) based on the wetted area of the prey, A_w is the wetted area of the prey (m^2), ρ is the density of the medium (kg m^{-3}) and FS is the speed of the fluid at the location of the object (m s^{-1}). For the range of Reynolds numbers Re=300–10 000 we used the drag coefficient measured for *Euphausia superba* (Kils, 1982). For the range of Reynolds numbers 10 000–85 000 (~0.25–3.6 m s^{-1}) we used empirically determined drag coefficients that we measured for live tethered shrimp, *Palaemonetes*, in a flume under conditions of steady, uniform flow over a range of flow speeds (see Denny et al., 1985). The shape of *E. superba* is similar to that of *Palaemonetes*, thus the drag coefficient is expected to be similar. Moreover, the data of Kils (Kils, 1982) can be combined with our measurements to produce the relationship of C_d=0.0708$Re^{-0.1703}$ (R^2=0.84), with Re calculated based on the prey's length.

Pressure gradient force (F_{pg}) was calculated as:

$$F_{pg} = (dp/dx) \times L_x \times A_f ,$$

where L_x is the effective dimension of each bin in the x-direction (0.002 m), A_f is the frontal area of the bin (m^2) and dp/dx is calculated from the spatial and temporal gradients of velocity using the momentum equation (as in Wainwright and Day, 2007).

Acceleration reaction force (F_{ar}) was calculated as:

$$F_{ar} = C_{am} \times V \times \rho \times a ,$$

where V is the volume of the bin (m^3), ρ is the density of the medium (kg m^{-3}) and a is the acceleration of the water surrounding the prey (m s^{-2}). The coefficient of added mass, C_{am}, was estimated based on our measured forces, by calculating expected force with added mass coefficients ranging from 0.3 to 1.0 [the range of C_{am} often measured for marine invertebrates (Daniel, 1984; Daniel and Meyhofer, 1989; Denny et al., 1985; Martinez, 2001)] and comparing the results to the observed force. That comparison was independently made at three time points: at the moment of peak force, at the moment of peak gape, and 2 ms after force initiation (where drag is supposed to be negligible due to the low flow speed). The added mass coefficient that resulted in a slope of X=Y at these three time points was 0.5, slightly higher than that of a more streamlined flexed carridean shrimp (C_{am}=0.4±0.09) (Daniel and Meyhofer, 1989). An added mass coefficient of 0.5 was used in all subsequent calculations.

The contribution of the transducer's rod to the observed forces was estimated by calculating the force exerted on a bare rod located in front of the fish, using the observed fish kinematics. The rod was treated as a 100 mm long cylinder, 0.3 mm in diameter, with its proximal end 4 mm posterior to the original location of the prey's eye. Drag and added mass coefficients were taken from Vogel (Vogel, 1994). The total calculated force was 2.6% (± s.d.=1.6%) of the total force

exerted on the prey. Our force measurements (observed values) were corrected accordingly.

Simulations

To test whether bluegill optimally positioned the prey relative to their mouth in each strike, we calculated the force that would have been exerted on the prey had the strike been initiated (and ended) at a range of different distances. For each strike, we used the observed kinematics (gape and mouth displacement, as well as prey size and peak flow velocity), but varied the strike initiation distance from 0.5 to 20 mm in 0.5 mm increments (corresponding to the observed range of strike initiation distances; see results). We then compared the observed strike starting distance with the distance that yielded the maximal simulated force, and calculated the ratio between the observed peak force and the maximal potential force (hereafter defined as 'force efficiency').

It could be that the fish were expecting the prey to dismount from the rod to which they were glued. Thus, the fish may have been coordinating their strikes to optimize the forces exerted on free (rather than an attached) prey. To test this alternative hypothesis, we modeled the force exerted on a free shrimp, for strikes starting at the same range of strike initiation distance (0.5–20 mm), using the observed kinematics of the fish. The path of the prey, however, was simulated as that of an unattached prey by calculating the expected movement of the prey according to the prey's mass and the force exerted on the prey at each time step (see Wainwright and Day, 2007). The distance yielding the highest force on the simulated 'free' prey was compared to the observed distance, and the force efficiency was also calculated.

Statistical analysis

Since we repeatedly measured the force exerted by four fish, these observations cannot be considered independent. The correspondence between observed values of peak force and those calculated based on the model was assessed using repeated-measures (RM) ANOVA (Rao, 1998) with fish as subjects, the difference between observed and calculated force for each strike as the dependent variable and strike sequential number as repeated-measure factor. A significant deviation between the model's results and observed forces was interpreted if the least square mean of the difference was significantly different than 0. A similar analysis was performed to test the relationship between observed and calculated time of peak forces. As an indicator for the model's precision in predicting the force on the prey, we also report the average slope and R^2 of regression between the magnitude and timing of the observed and calculated force (as well as other variables), made separately for each of the four fish used in the experiment. Note that these statistics should be viewed as descriptive statistics, since repeated force measurements for each fish are not independent. The deviation of each observed strike initiation distance from the distance associated with maximum potential force (calculated from our simulations) was used as a metric of 'strike precision'. Variation in strike precision for fixed and free prey was tested using RM-ANOVA with fish as subjects, strike precision as the dependent variable and strike sequential number as the repeated-measured factor. If no difference in precision between the four fish was observed, the overall least square mean was taken as the measure of strike precision. The sphericity assumption was verified prior to running RM-ANOVA. Linear regression is reported after verifying normal distribution of the residuals. All the parametric and non-parametric tests were performed using JMP IN version 5.0 (SAS institute, NC, USA).

Results

Empirical force measurements

The peak force produced during strikes by bluegill ranged from 0.005 to 0.506 N (mean ± s.d.=0.177±0.13 N; N=48). Force was initiated, on average, 5.6±7.9 ms after the start of mouth opening and peaked 6.1±6.5 ms after peak gape (Fig. 2A). When normalized by TTPG (time as fraction of TTPG), force was initiated about halfway through the gape cycle (0.45±0.32 TTPG cycles after gape initiation) and peaked 0.55 (±0.38) TTPG cycles after peak gape (Fig. 2B). Prey entered the mouth at, or within 2 ms of peak gape. The difference between the time it took the fish to achieve full gape (TTPG; average of 12.2 ms) and the time from force initiation to peak force (average 13.02 ms) was not significantly different from 0 (indicated by the overall least square mean in RM-ANOVA; $F_{1,3}$=2.8, P>0.1), and the durations of the two were correlated (Pearson r=0.48, P<0.05). TTPG and prey length, but not strike initiation distance, affected the magnitude of peak force (multiple regression, whole model R^2=0.47). Peak force was negatively correlated with strike initiation distance (R^2=0.15 between the residuals of peak force and strike initiation distance) while prey length and TTPG were positively correlated with peak force (R^2=0.21 between residuals of peak force and prey diameter. The single variable that best explained the observed trends in peak force was TTPG (R^2=0.42; Fig. 3). However for any given TTPG, observed force varied up to fivefold (Fig. 3).

Strike kinematics

Strikes differed in their kinematics, including TTPG (range 6–26 ms; Fig. 3, Fig. 4A), strike initiation distance (range 0–18.5 mm; Fig. 4B), mouth displacement (range 3–18.5 mm;

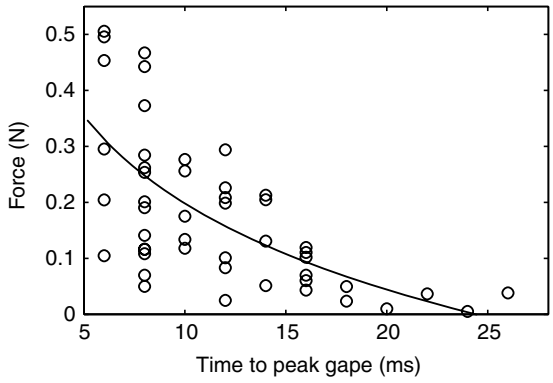

Fig. 3. The force exerted on attached shrimp as a function of TTPG (the speed of buccal expansion). Note that for a given strike effort (TTPG) there is considerable variation in force. The relationship between the observed force and TTPG is given by the equation: peak observed force=2.35×TTPG^{-1}–0.05 (R^2=0.42; solid line).

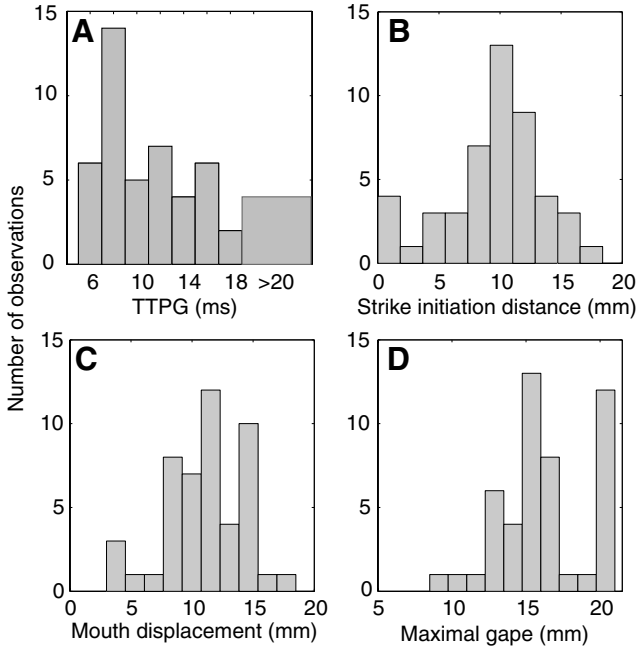

Fig. 4. Variability in prey capture kinematics in bluegill striking tethered shrimp. (A) Time to peak gape (TTPG); (B) strike initiation distance; (C) mouth displacement; (D) maximal gape width. N=48 strikes, 12 per fish. Strike initiation distance and mouth displacement were correlated (R^2=0.62, P<0.001) while no correspondence was found between the other variables.

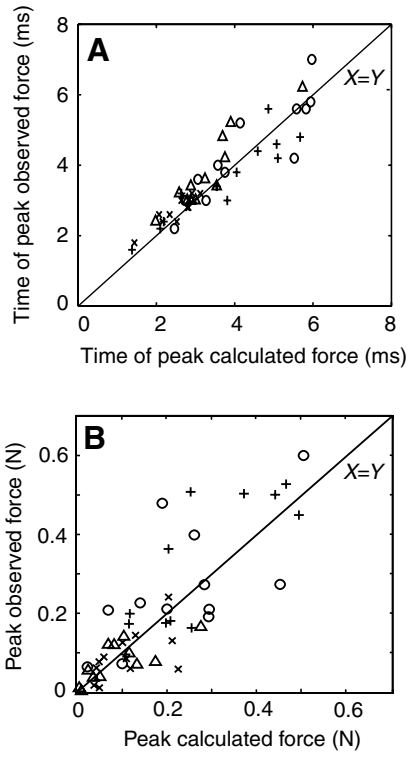

Fig. 5. Comparison of timing (A) and magnitude (B) of the observed and calculated forces exerted by bluegill on tethered prey. Time 0 (in B) is the first frame digitized in the image sequence (~10 frames prior to the onset of gape, arbitrarily selected for each sequence). The timing differences between the observed and calculated peak force were not significantly different than 0 (average 2.2±0.83 ms; RM-ANOVA $F_{1,3}$=3.76, P>0.15) and were linearly correlated (average R^2=0.78±0.06; average slope=0.89±0.09; N=4 fish). Similarly, the peak calculated force was not significantly different than the observed one (average deviation=–0.012±0.135 N; RM-ANOVA $F_{1,3}$=0.45, P>0.54) and the two magnitudes were correlated (average R^2=0.59±0.07; average slope=0.78±0.1; N=4 fish). Different symbols represent data for the four fish studied, diagonal line represents the case of X=Y.

Fig. 4C) and maximal gape width (8.5–21 mm; Fig. 4D). Strikes that were initiated at a greater distance from the prey were characterized by greater mouth displacement (linear regression R^2=0.62, $F_{1,46}$=78.5, P<0.001). No correlation was observed between the other variables (Pearson correlation, P>0.05 for all cases).

Comparisons with calculated forces

While TTPG and prey length affected the magnitude of peak force in a multiple linear regression (see above), this linear model ignores possible non-linear effects of the independent variables on the force, which can be derived from theory. Therefore, we studied the effect of the kinematic variables using a mechanistic model (Wainwright and Day, 2007). The magnitude and timing of the observed forces exerted on the tethered shrimps were in good agreement with those expected based on the model (Fig. 5A,B). The average deviation between the timing of the observed and calculated peak forces was not significantly different from 0 (average 2.2±0.83 ms; indicated by the overall least square mean in RM-ANOVA; $F_{1,3}$=3.76, P>0.15). There was no effect of strike order (sequential number) on the difference in timing of observed and expected peak force (RM-ANOVA; $F_{11,33}$=1.03, P>0.45). Similarly, the average deviation between the magnitude of the peak observed and calculated forces was not significantly different from 0 (average –0.012±0.135 N; indicated by the overall least square mean in RM-ANOVA; $F_{1,3}$=0.45, P>0.54) with no effect of strike order (sequential number) on the difference in magnitude between observed and expected force (RM-ANOVA; $F_{11,33}$=0.9, P>0.54). Calculated peak forces exerted on prey were strongly correlated with observed forces (average R^2=0.59±0.07; N=4 fish; Fig. 5B) and the average slope was 0.78±0.1 (N=4 fish). Similarly, the timings of the observed and calculated peak forces were linearly correlated (average R^2=0.78±0.06; N=4 fish; Fig. 5A) and the average slope was 0.89±0.09 (N=4 fish).

The strongest force exerted on the shrimp was the pressure gradient force (65.7±1.6% of the force at the time of peak force; Fig. 6), followed by acceleration reaction force (32.9±3.3%) and drag force (1.4±3.3%). Thus, fast acceleration of the water in front of the mouth has a much stronger effect on force than the fluid speed. Peak drag occurred 4.1 ms (±3.5 ms) after peak force, while pressure gradient force and acceleration reaction peaked simultaneously at 0.3±1.4 ms before peak force (Fig. 6).

Simulations of strike initiation distance

The good fit between calculated and observed forces allowed us to simulate strikes and explore the effects of variation in

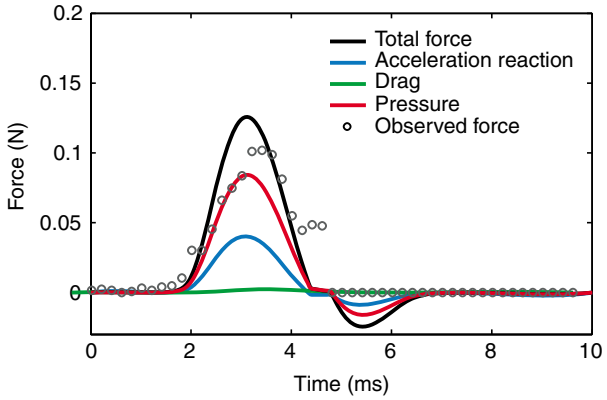

Fig. 6. Representative sequence of observed force (open circles), and the calculated forces due to acceleration reaction (blue line), drag (green line) and pressure gradient (red line). The three calculated forces sum to total calculated force (black line). Note that pressure gradient force (an average of 65.7% of total force) and acceleration reaction force (32.9%) peak concurrently, while drag force (1.4%) peaks ~0.7 ms later. The observed and calculated forces are in good agreement throughout the strike (R^2=0.84, P<0.001).

strike initiation distance. Altering strike initiation distance, and thereby changing the position of the prey at the moment of peak flow, resulted in a concave response of peak force (Fig. 7), with maximal peak force achieved within the simulated range (0.5–20 mm) for all strikes. The average force efficiency, defined here as the ratio between peak force at the observed distance and the highest simulated force, was 0.706±0.045 (average for N=4 fish). The average deviation between the observed distance and the distance of maximal force, indicated by the overall least square mean in RM-ANOVA, was not significantly different from 0 (average 1.9±3.6 mm; $F_{1,3}$=2.9, P>0.1). The distance associated with the maximal peak force was linearly correlated with the observed distance (average R^2=0.49±0.25; N=4 fish; Fig. 8) and the average slope was 0.85±0.22 (N=4 fish). There was no correlation between strike precision and observed force (Spearman rank correlation, P>0.1), and fish did not improve in strike precision through the experiment (RM-ANOVA, $F_{11,33}$=0.7, P>0.1).

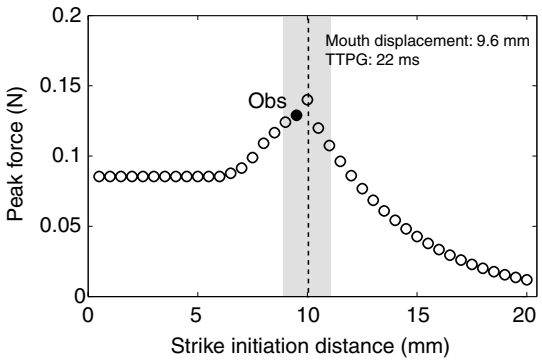

Fig. 7. The simulated change in calculated peak force (open circles) as a function of strike initiation distance in a representative strike. Force was modeled based on original strike kinematics, with strike initiation distance systematically changed from 0.5–20 mm in 0.5 mm increments. Grey shaded region is the 90% force efficiency zone, in which peak force for each simulated strike was ⩾90% of the maximal force within the simulated range. The observed strike initiation distance for this sequence is also noted (9.6 mm; filled circle; marked 'Obs'). The flow speed within the buccal cavity was assumed equal to that at the mouth aperture, hence the flat response of peak force at short strike-initiation distances.

In addition to peak force, fish could potentially maximize the rate of increasing force, defined as the slope of increasing force from force onset to peak force. Although the strike initiation distance that resulted in maximum slope was correlated with the distance of maximal force, the latter was closer to the mouth, and the fit between the observed distance and that corresponding to the highest slope was weak (average R^2=0.33±0.1; N=4 fish).

To test the hypothesis that the fish were optimizing their kinematics for a free-swimming prey, rather than attached prey, we calculated the distance associated with the highest force for such prey. As in the case of attached prey, altering strike initiation distance resulted in a concave response of peak force (data not shown). Maximal peak force exerted on the prey in this scenario was much lower than that on attached prey, because the prey was modeled to move with the water [hence the relative acceleration and speed are small (Wainwright and Day, 2007)]. The distance associated with maximal force exerted on a free prey was (on average) 85±20% longer than that observed, with a higher deviation (5.5±3.0 mm, intercept in RM-ANOVA significantly different than 0; $F_{1,3}$=120, P<0.001) and a poorer fit with the observed distance (average R^2=0.26±0.1; N=4 fish). Strike efficiency, however, was similar to that of attached prey (0.71±0.09).

Discussion

Suction feeders generate a flow of water in front of their mouth that is used to transport prey into the oral cavity. That

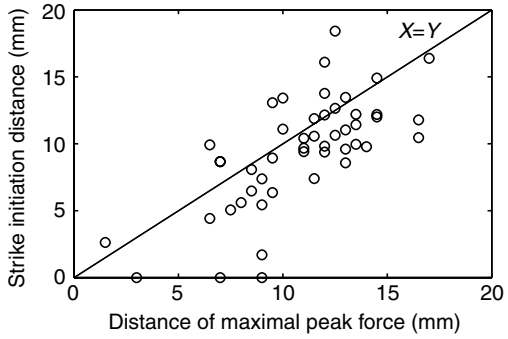

Fig. 8. Strike precision in bluegill. Observed strike starting distance is the distance between the prey's eye and the center of the fish's mouth at the moment of strike initiation (initiation of gape expansion). The distance of maximal force was estimated by calculating the expected force achieved, with the observed kinematics, for strike starting distances between 0.5 and 20 mm, in 0.5 mm intervals. The distance of maximal force (defined as the distance associated with the highest peak force) was not significantly different than the observed strike initiation distance (average 1.9±3.6 mm; RM-ANOVA $F_{1,3}$=2.9, P>0.1). The distance associated with the maximal peak force was linearly correlated with the observed distance (average R^2=0.49±0.25; average slope=0.85±0.22; N=4 fish). Diagonal line represents the case of X=Y.

flow generates a net force that tends to draw the prey into the mouth, and the magnitude of this force is likely to be an important component of overall suction feeding performance. In cases were the prey exerts force in the opposite direction by being attached to the substrate (or by swimming, in the case of escaping prey), exerting higher forces on prey increases the probability of the predator capturing the prey. Therefore, there should be strong selection for feeding kinematics that maximizes that force. As faster fluid acceleration is directly associated with higher acceleration reaction and pressure gradient forces, acceleration should be viewed as the primary mechanism for enhancing the force exerted on the prey. However, bluegill were also precise in positioning themselves very close to the distance of maximal peak force, but fell far short of producing the highest possible rate of increasing force. These results highlight the importance of precision during suction feeding in fishes, and the important role of coordination between each strike's unique kinematics and starting distance.

The observed strike starting distance was correlated with the distance associated with highest force exerted on an attached prey, but not on a free prey. This comparison indicates that the fish, being trained to feed from the transducer, adapted their kinematics according to this feeding mode. Moreover, different prey behaviors (attached and free prey) result in different solutions that optimize the force on the prey, because the trajectory of the prey during a strike is different. Bluegill are also known to encounter prey that display escape responses [such as copepods and shrimps (VanderKooy et al., 2000)] that are triggered by the hydromechanical disturbances created by the suction feeding fish (Arnott et al., 1999; Fields and Yen, 1997). Both the bow wave in front of the approaching fish and the slower flow produced during the early stages of the strike can stimulate an escape response from the prey. In this situation, the relative velocity, escape trajectory and timing of the response can be critical in determining the outcome of the interaction (Howland, 1974). For example, the optimal strike starting distance can be expected to vary according to the prey's sensitivity and the timing of its escape response. However, investigation of interactions between fish and their prey often ignore the effect of suction forces on the prey's trajectory (e.g. Arnott et al., 1999; Fields and Yen, 1997; Howland, 1974; Weihs and Webb, 1984).

Morphological adaptations that are used to increase intra-oral pressure (and thereby fluid speed) in centrarchids include an increase in the cross section area of epaxial muscles, changes in the lever system that controls the rotation of the neurocranium (Carroll et al., 2004), and reduced mouth size (Carroll et al., 2004; Wainwright and Day, 2007). Behavioral modifications recognized to enhance the forces exerted by suction feeders have previously been limited to increased flow by increasing the rate of buccal expansion (Day et al., 2005; Wainwright and Day, 2007). Under the same rate of buccal expansion (i.e. same flow speed at the mouth) the effects of head kinematics on either intra-oral pressure (Nemeth, 1997) or modeled flow speed outside the mouth (Van Wassenbergh et al., 2006) have been considered insignificant, except for the timing of opening the opercular slits (Van Leeuwen and Muller, 1984). However, the fact that there is a fivefold range in force exerted on the prey in strikes with a similar strike effort and flow speed may indicate the ability to generate high flow speed is insufficient to exert high force on the prey. Proper positioning of the prey in the narrow region of high flow speed in front of the mouth, during the short time period in which high flow persists, may also be required to optimize the effects of the flow on the prey. Modulation of strike kinematics, through strike starting distance or the extent of mouth displacement, are possible ways by which suction feeding fish can optimize their performance. Throughout our experiments, strikes performed by the same fish on the same prey frequently showed very different kinematics. Even though experimental conditions were fixed, convergence for a single solution was not observed. This observation may indicate that there is more than one solution for an optimized strike at any given strike effort. However, the chosen kinematics appears to be a non-random subset, coordinated with initiation distance and prey behavior.

The concave response of maximal peak force with increasing strike initiation distance (Fig. 7 for attached prey; similar results for free prey not shown), supports the hypothesis of a strike-specific position of maximal efficiency, spanning only a few mm. Gauging the initiation distance of the strike is likely to involve visual feedback and may be an underappreciated function of vision in suction feeders. The keen visual acuity of bluegill relative to other centrarchids has previously only been linked to prey detection (e.g. Hairston et al., 1982; Hawryshyn et al., 1988).

In this study we were able to accurately predict the forces exerted on the prey, based on a suite of kinematic measurements (jaw kinematics and the distance from the prey). This was possible due to the tight link between kinematics and flow speed in front of the bluegill's mouth (Day et al., 2005) and our understanding of the nature of the forces exerted on an object in a suction feeding flow (Wainwright and Day, 2007). It is a major goal in organismal biomechanics to measure the forces that are exerted on animals during locomotion and feeding (e.g. Peng et al., 2007; Van Wassenbergh et al., 2006; Vogel, 1994). For animals in a fluid environment, however, it is usually difficult to measure these forces directly. Here we took advantage of the presence of a prey in the flow field to combine fluid mechanical calculations with empirical measurements, and to further use the mechanics to test the fish's performance in an ecologically relevant scenario. The current understanding of the effect of water flow on the prey can be used to calculate the forces exerted on prey in other scenarios, such as escaping prey, neutrally buoyant detached prey or heavy attached prey. These are all ecologically relevant scenarios, which may represent a fish striking on an escaping shrimp, a fish egg, and a snail, respectively. This model can also be used to examine the effects of inter-specific morphological and behavioral variability on suction feeding performance, a highly time consuming and demanding task if approached by empirical methods.

The force exerted by an aquatic suction feeding fish on its prey was measured here for the first time. As a suction feeding specialist, bluegill carefully time their strike and exert high, abrupt forces on their prey. Future research can now begin to make comparisons of the ability of different species to exert force on their prey, and because these forces depend intimately on the details of prey capture kinematics, suction feeding is emerging as a model behavior in which the ability of organisms

to coordinate aspects of their movement can be directly and mechanistically tied to performance.

We thank Tim Higham who contributed to the early stages of this project, and Rita Mehta for critical comments on an earlier draft of the manuscript. We are especially grateful to Mike Boller and Mark Denny for their expertise and creativity in helping us measure the drag coefficient of shrimp. Comments made by two anonymous reviewers helped us refine the model and improved the manuscript. Support for this research was provided by National Science Foundation grants 0444554 and 0610310.

References

Arnott, S. A., Neil, D. M. and Ansell, A. D. (1999). Escape trajectories of the brown shrimp *Crangon crangon*, and a theoretical consideration of initial escape angles from predators. *J. Exp. Biol.* **202**, 193-209.

Batchelor, G. K. (1967). *An Introduction to Fluid Mechanics*. Cambridge: Cambridge University Press.

Carroll, A. M., Wainwright, P. C., Huskey, S. H., Collar, D. C. and Turingan, R. G. (2004). Morphology predicts suction feeding performance in centrarchid fishes. *J. Exp. Biol.* **207**, 3873-3881.

Coughlin, D. J. and Strickler, R. J. (1990). Zooplankton capture by a coral reef fish: an adaptive response to evasive prey. *Environ. Biol. Fishes* **29**, 35-42.

Daniel, T. L. (1984). Unsteady aspects of aquatic locomotion. *Am. Zool.* **24**, 121-134.

Daniel, T. L. and Meyhofer, E. (1989). Size limits in escape locomotion of Carridean shrimp. *J. Exp. Biol.* **143**, 245-265.

Day, S. W., Higham, T. E., Cheer, A. Y. and Wainwright, P. C. (2005). Spatial and temporal patterns of water flow generated by suction-feeding bluegill sunfish *Lepomis macrochirus* resolved by Particle Image Velocimetry. *J. Exp. Biol.* **208**, 2661-2671.

Denny, M. W. (1988). *Biology and the Mechanics of the Wave-Swept Environment*. New Jersey: Princeton University Press.

Denny, M. W., Daniel, T. L. and Koehl, M. A. R. (1985). Mechanical limits to size in wave-swept organisms. *Ecol. Monogr.* **55**, 69-102.

Ferry-Graham, L. A., Wainwright, P. C. and Lauder, G. V. (2003). Quantification of flow during suction feeding in bluegill sunfish. *Zoology* **106**, 159-168.

Fields, D. M. and Yen, J. (1997). The escape behavior of marine copepods in response to a quantifiable fluid mechanical disturbance. *J. Plankton Res.* **19**, 1289-1304.

Flemer, D. A. and Woolcott, W. S. (1966). Food habits and distribution of the fishes of Tuckahoe Creek, Virginia, with special emphasis on the bluegill, *Lepomis macrochirus* Rafinesque. *Chesapeake Sci.* **7**, 75-89.

Gibb, A. C. and Ferry-Graham, L. (2005). Cranial movements during suction feeding in teleost fishes: Are they modified to enhance suction production? *Zoology* **108**, 141-153.

Gillis, G. B. and Lauder, G. V. (1995). Kinematics of feeding in bluegill sunfish: is there a general distinction between aquatic capture and transport behaviors? *J. Exp. Biol.* **198**, 709-720.

Hairston, N. G., Jr, Li, K. T. and Easter, S. S., Jr (1982). Fish vision and the detection of planktonic prey. *Science* **218**, 1240-1242.

Hawryshyn, C. W., Arnold, M. G., McFarland, W. N. and Loew, E. R. (1988). Aspects of color vision in bluegill sunfish (*Lepomis Macrochirus*): Ecological and evolutionary relevance. *J. Comp. Physiol. A* **164**, 107-116.

Higham, T. E., Day, S. W. and Wainwright, P. C. (2005). Sucking while swimming: evaluating the effects of ram speed on suction generation in bluegill sunfish *Lepomis macrochirus* using digital particle image velocimetry. *J. Exp. Biol.* **208**, 2653-2660.

Higham, T. E., Day, S. W. and Wainwright, P. C. (2006a). Multidimensional analysis of suction feeding performance in fishes: fluid speed, acceleration, strike accuracy and the ingested volume of water. *J. Exp. Biol.* **209**, 2713-2725.

Higham, T. E., Day, S. W. and Wainwright, P. C. (2006b). The pressures of suction feeding: the relation between buccal pressure and induced fluid speed in centrarchid fishes. *J. Exp. Biol.* **209**, 3281-3287.

Howland, H. C. (1974). Optimal strategies for predator avoidance – relative importance of speed and maneuverability. *J. Theor. Biol.* **47**, 333-350.

Huish, M. T. (1957). Food habits of three centrarchidae in Lake George, Florida. *Proc. Annu. Conf. S. E. Assoc. Game Fish Comm.* **11**, 293-302.

Kils, U. (1982). Swimming behavior, swimming performance and energy balance of antarctic krill *Euphausia superba*. *BIOMASS Sci. Ser.* **3**, 1-233.

Martinez, M. M. (2001). Running in the surf: hydrodynamics of the shore crab *Grapsus tenuicrustatus*. *J. Exp. Biol.* **204**, 3097-3112.

Muller, M., Osse, J. W. M. and Verhagen, J. H. G. (1982). A quantitative hydrodynamical model of suction feeding in fish. *J. Theor. Biol.* **95**, 49-79.

Nauwelaerts, S., Wilga, C., Sanford, C. and Lauder, G. V. (2007). Hydrodynamics of prey capture in sharks: effects of substrate. *J. R. Soc. Interface* **4**, 341-345.

Nemeth, D. H. (1997). Modulation of buccal pressure during prey capture in *Hexagrammos decagrammus* (Teleostei: Hexagrammidae). *J. Exp. Biol.* **200**, 2145-2154.

Norton, S. F. (1991). Capture success and diet of Cottid fishes – the role of predator morphology and attack kinematics. *Ecology* **72**, 1807-1819.

Peng, J., Dabiri, J. O., Madden, P. G. and Lauder, G. V. (2007). Non-invasive measurement of instantaneous forces during aquatic locomotion: a case study of the bluegill sunfish pectoral fin. *J. Exp. Biol.* **210**, 685-698.

Rao, P. V. (1998). *Statistical Research Methods in the Life Science*. Belmont, CA: Duxbury Press.

Sadzikowski, M. R. and Wallace, D. C. (1976). A comparison of the food habits of size classes of three sunfishes (*Lepomis macrochirus* Rafinesque, *Lepomis gibbosus* (Linnaeus) and *Lepomis cyanellus* Rafinesque). *Am. Midl. Nat.* **95**, 220-225.

Sanford, C. P. J. and Wainwright, P. C. (2002). Use of sonomicrometry demonstrates link between prey capture kinematics and suction pressure in largemouth bass. *J. Exp. Biol.* **205**, 3445-3457.

Van Leeuwen, J. L. and Muller, M. (1984). Optimum sucking techniques for predatory fish. *Trans. Zool. Soc. Lond.* **37**, 137-169.

Van Wassenbergh, S., Aerts, P. and Herrel, A. (2006). Hydrodynamic modelling of aquatic suction performance and intra-oral pressures: limitations for comparative studies. *J. R. Soc. Interface* **3**, 507-514.

VanderKooy, K. E., Rakocinski, C. F. and Heard, R. W. (2000). Trophic relationships of three sunfishes (*Lepomis* spp.) in an estuarine bayou. *Estuaries* **23**, 621-632.

Vogel, S. (1994). *Life in Moving Fluids*. Princeton: Princeton University Press.

Wainwright, P. C. and Day, S. W. (2007). The forces exerted by aquatic suction feeders on their prey. *J. R. Soc. Interface* **4**, 553-560.

Wainwright, P. C., Ferry-Graham, L. A., Waltzek, T. B., Carroll, A. M., Hulsey, C. D. and Grubich, J. R. (2001). Evaluating the use of ram and suction during prey capture by cichlid fishes. *J. Exp. Biol.* **204**, 3039-3051.

Weihs, D. and Webb, P. W. (1984). Optimal avoidance and evasion tactics in predator-prey interactions. *J. Theor. Biol.* **106**, 189-206.